Journal of Inflammation Research

Dovepress
open access to scientific and medical research

Open Access Full Text Article

ORIGINAL RESEARCH

RNA Sequencing Analyses Reveal the Potential Anti-Inflammatory Mechanisms of Acacetin Against ODG/R Injuries in Microglia

Juan Bu[1], Yeledan Mahan[1], Yanmin Zhang[2], Shengnan Zhang[1], Xuanxia Wu[1], Xiaoling Zhang[1], Ling Zhou[1]

[1]Medical and Translational Research Center, People's Hospital of Xinjiang Uygur Autonomous Region, Urumqi, Xinjiang, People's Republic of China; [2]Scientific Research and Education Center, People's Hospital of Xinjiang Uygur Autonomous Region, Urumqi, Xinjiang, People's Republic of China

Correspondence: Ling Zhou, Medical and Translational Research Center, People's Hospital of Xinjiang Uygur Autonomous Region, 91 Tianchi Road, Tianshan District, Urumqi, Xinjiang, 830001, People's Republic of China, Tel +86 991 8562 317, Email zlrmyy@sina.com

Background: Acacetin is a natural flavonoid known for its anti-tumor, antioxidant, and anti-inflammatory properties. Our previous studies have shown its protective effects against cerebral ischemia-reperfusion injury (IRI), but the underlying molecular mechanisms remain unclear.

Purpose: The study delves into acacetin's mechanism in mitigating cerebral IRI, with a focus on transcriptomic insights.

Methods: We established the oxygen-glucose deprivation/re-oxygenation (OGD/R) model in BV2 microglia, treating them with 10μM acacetin. Then we assessed cell proliferation using CCK-8 and measured Lactate Dehydrogenase (LDH) release. High-throughput RNA sequencing (RNA-seq) underpinned the analysis of differentially expressed genes (DEGs) and long non-coding RNAs (lncRNAs), functional enrichment, and alternative splicing events (ASEs), validated by reverse transcription–quantitative polymerase chain reaction (RT-qPCR).

Results: OGD/R injury significantly impaired cell proliferation and increased LDH release, effects mitigated by acacetin. RNA-seq identified 2148 upregulated and 2135 downregulated DEGs post-OGD/R. In contrast, the acacetin-treated group showed 248 upregulated and 240 downregulated DEGs compared to the OGD/R group. All DEGs were enriched in both Gene Ontology (GO) terms and Kyoto Encyclopedia of Genes and Genomes (KEGG) pathways. Overlapping analysis indicated that acacetin treatment reversed the expression of 203 genes affected by OGD/R, including inflammation-related genes such as Isg15, Fcgr1, Il1b, and Parp12. Moreover, the oxidative stress-related gene, Mt2, was downregulated post-OGD/R but upregulated following acacetin treatment. We further found that OGD/R and acacetin treatment could modulate gene splicing events, impacting cell apoptosis or inflammatory responses, such as the A3SS splicing event in the Trim47 gene. RNA-seq also highlighted differential expression of numerous lncRNAs, particularly the upregulation of lncRNA Rmrp and Terc post-OGD/R and their subsequent downregulation post-acacetin treatment. These lncRNAs might regulate cell proliferation through mediating target gene expressions. RT-qPCR validation confirmed these findings.

Conclusion: Significant upregulation of genes and ASEs linked to oxidative stress and inflammatory response is observed in cerebral IRI. Acacetin intervention reverses these effects, highlighting its mechanism in alleviating the injury by modulating gene expression and splicing events.

Keywords: acacetin, ischemic stroke, inflammation, genome-wide analysis, differentially expressed genes, alternative splicing, long non-coding RNA, RNA sequencing

Introduction

Stroke, also referred to as cerebral vascular accident or brain attack, is a severe cerebrovascular disease characterized by considerable incidence, morbidity, mortality, and recurrence rates. With changes in socio-economic structures and disease patterns, stroke has become the leading cause of disability and death in China, displaying an increasing trend and

Received: 21 February 2024
Accepted: 29 May 2024
Published: 5 June 2024

affecting younger populations. According to a report from the China Stroke Center, among adults aged 40 years and older, the estimated overall prevalence and incidence in 2020 were 2.6% and 505.2 per 100,000 person-years, respectively. Notably, ischemic strokes accounted for 71.55% of these cases.[1] It indicates 17.8 million cases of stroke and 3.4 million new strokes in China, costing the nation about 400 billion yuan annually. Ischemic stroke not only severely impacts people's health and quality of life but also imposes a substantial medical, economic, and social burden on both the nation and families, marking it as a critical public health issue.

Following the onset of an ischemic stroke, there is a marked increase in reactive free radicals, which in turn activates cerebral inflammatory cells. Then it leads to the extensive secretion of pro-inflammatory cytokines and reactive oxygen species (ROS), triggering cellular necrosis and apoptosis in the lesion region.[2] As the resident innate immune cells of the brain, microglia are the earliest responders to cerebral ischemic injury and participate in the pathophysiological process of ischemic stroke.[3] Thus, a deeper understanding of pathogenesis of microglia after ischemia stroke at the molecular and genetic levels, along with the identification of effective biological targets and therapeutic agents, is essential for the prevention and treatment of ischemic stroke.

Acacetin, a flavonoid compound, can be extracted from various plants, including *Saussurea involucrata*, acacia, and chrysanthemums. Our previous study found that acacetin can inhibit inflammatory responses and exert protective effects against ischemic stroke in both in vitro and in vivo experiments, yet the specific mechanisms require further research.[4] With the development of RNA sequencing (RNA-seq) technology, transcriptome analysis is increasingly applied in understanding the pathogenesis of ischemic stroke, enhancing clinical diagnosis, and advancing pharmacological studies.[5,6]

We hypothesized that acacetin protects against ischemic stroke by regulating gene expression and alternative splicing, thereby affecting genes involved in oxidative stress and neuroinflammation. Hence, we established three cell models: untreated (normal) cells, cells treated with Oxygen-Glucose Deprivation/Reperfusion (OGD/R), and cells intervened with acacetin post-OGD/R. Cell viability was assessed using the CCK-8 assay, while LDH release was evaluated with the LDH assay kit. High-throughput RNA-seq was used to identify differentially expressed mRNA and long non-coding RNA (lncRNA), and alternative splicing events (ASEs) among the three cell models. The differentially expressed genes (DEGs) identified were validated by reverse transcription–quantitative polymerase chain reaction (RT-qPCR).

Material and Methods

Cell Culture

The cell experiments were conducted from February 2023 at the Central Laboratory of the People's Hospital of Xinjiang Uygur Autonomous Region. BV2 cells (CX0103, Boster, Wuhan, China) were cultured in a high-glucose DMEM complete medium (SH30022.01, HyClone, United States) supplemented with 10% Fetal Bovine Serum (FBS, SH30406.05, HyClone, New Zealand), penicillin, and streptomycin and maintained in an incubator at 37°C with 5% CO_2. Once the cells reached a confluency of 80%, they were subcultured. Cells in the logarithmic growth phase with good conditions were selected for experiments. The cells were divided into a control group, an OGD/R model group, and an OGD/R group intervened with acacetin (10 μM, 00017, Sigma, United States). For the preparation of the acacetin intervention, it was diluted in 0.1% dimethyl sulfoxide (DMSO, D8371, Solarbio, Beijing, China).

OGD/R Model Establishment and Acacetin Intervention

The OGD/R model was prepared following a method described in another study.[7] For the OGD/R model group and the acacetin intervention group, the DMEM medium containing 10% FBS was replaced with glucose-free DMEM medium (11,966,025, Gibco, United States) and then incubated in a pre-set incubator (1% O_2, 5% CO_2, and 94% N_2) for 4 hours. The control group was continuously cultured under regular conditions. The acacetin intervention group was treated with 10 μM acacetin in the culture medium 30 mins before OGD/R, during OGD/R, and 24 hours post-OGD/R. After the OGD/R process, cells from all groups were simultaneously retrieved, and the culture medium was replaced with DMEM containing 10% FBS. They were then returned to a 37°C incubator with 5% CO_2 and cultured for 24 hours to simulate reperfusion.

CCK-8 Assay

BV2 cells seeded in 96-well plates and subjected to the corresponding pre-treatments were used for the CCK-8 assay (K1018, APExBIO, United States). Wells containing only culture medium without cells were set as control wells. 10 μL of CCK-8 solution was added to each well, followed by incubation in a culture incubator for 1 hr. The absorbance was measured at 450 nm using a microplate reader. Cell viability rate = [(optical density (OD) value of test group – OD value of blank group) / (OD value of control group – OD value of blank group)] × 100%.

LDH Release Assay

After 24 hours of re-oxygenation, the supernatant from the cell culture was collected. 60 μL of LDH detection working solution (C0016, Beyotime, Shanghai, China) was added to each well, mixed well, and then incubated at room temperature in the dark for 30 mins. After the incubation period, the absorbance was measured at 490 nm. Cell mortality rate (%) = [(OD value of treated sample - OD value of sample control well) / (OD value of maximal enzyme activity - OD value of sample control well)] × 100%.

RNA Extraction and Sequencing

Total RNA was treated with RQ1 DNase (Promega) to remove DNA. The quality and quantity of the purified RNA were determined by measuring the absorbance at 260nm/280nm (A260/A280) using smartspec plus (BioRad). RNA integrity was further verified by 1.5% agarose gel electrophoresis.

For each sample, 1 μg of total RNA was treated with RQ1 DNase (Promega) to remove DNA before being used for directional RNA-seq library preparation by VAHTS® Universal V8 RNA-seq Library Prep Kit for Illumina (N605) for RNA-seq library preparation. mRNAs were captured by VAHTS mRNA capture Beads (Vazyme, N401) or Ribosomal RNAs were depleted with Ribo-off ™ rRNA depletion kit (Vazyme, N406-01). Fragmented mRNAs were converted into double-strand cDNA. Following end repair and A tailing, the DNAs were ligated to VAHTS RNA Multiplex Oligos Set 1 for Illumina (N323). The ligated products were amplified, purified, quantified, and stored at −80°C before sequencing. The strand marked with dUTP (the 2nd cDNA strand) is not amplified, allowing strand-specific sequencing.

For high-throughput sequencing, the libraries were prepared following the manufacturer's instructions and applied to Illumina Novaseq 6000 system for 150 nt paired-end sequencing.

RNA-Seq Raw Data Clean and Alignment

Raw reads containing more than 2-N bases were first discarded. Then adaptors and low-quality bases were trimmed from raw sequencing reads using FASTX-Toolkit (Version 0.0.13). The short reads less than 16nt were also dropped. After that, clean reads were aligned to the GRCm39 genome by HISAT2 allowing 4 mismatches.[8] Uniquely mapped reads were used for gene reads number counting and FPKM calculation (fragments per kilobase of transcript per million fragments mapped).[9]

Differentially Expressed Genes (DEGs) Analysis

The R Bioconductor package DESeq2 was utilized to screen out DEGs.[10] The P value <0.05 and fold change>1.5 or < 0.67 were set as the cut-off criteria for identifying DEGs.

Alternative Splicing Analysis

Regulatory alternative splicing events (RASEs) were defined and quantified using the SUVA pipeline.[11] The different splicing of each group was analyzed. Reads proportion of SUVA AS event (pSAR) of each AS events were calculated.

New Transcripts Predict Assembly

Group the RNA-Seq data, use stringtie to assemble the data of each group and predict the transcripts, screen the expression of the predicted transcripts of each group, eliminate the transcripts with FPKM< 1, and then use stringtie to combine them into one transcript (GTF file).[12]

lncRNA Prediction

In order to predict credible lncRNA, we used four software to predict lncRNA: CPC2, LGC, CNCI and CPAT.[13–16] We counted the noncoding transcripts identified by the above four analysis software. After the above steps, we successively removed the transcripts that overlap with the known coding genes, are less than 200bp in length, have potential coding ability, and are less than 1000bp away from the nearest gene from the assembly results, obtained the prediction results of new processing.

lncRNA Cis-Regulatory Target

Set the threshold of co-location as 100kb upstream and downstream of lncRNA in the trans-regulatory relationship pair, and then calculate the Pearson correlation coefficient between lncRNA and mRNA of co-location for co-expression analysis to screen the lncRNA target relationship pairs that meet the absolute value of correlation number greater than 0.6 and P value < = 0.01.[17] Then take the intersection of the two data sets of co-location and co expression to obtain the cis target of lncRNA.

Functional Enrichment Analysis

Gene Ontology (GO) terms and Kyoto Encyclopedia of Genes and Genomes (KEGG) pathways were identified using the KOBAS 2.0 server to sort out functional categories of DEGs.[18] Hypergeometric test and Benjamini-Hochberg FDR controlling procedure were used to define the enrichment of each term.

RT-qPCR

cDNA synthesis was done by reverse transcription kit (R323-01, Vazyme, China) at 42°C for 5min, 37°C for 15min, 85°C for 5seconds performed on the thermocycler (T100, Bio-Rad, USA). QPCR was performed on the ABI QuantStudio 5, followed by denaturing at 95°C for 10 min, 40 cycles of denaturing at 95°C for 15 sec, and annealing and extension at 60°C for 1 min. Each sample had three technical replicates. The concentration of each transcript was then normalized to GAPDH (glyceraldehyde-3-phosphate dehydrogenase) and mRNA level using the $2^{-\Delta\Delta Ct}$ method.[19] Comparisons were performed with the two-way ANOVA or the paired Student's *t*-test by using GraphPad Prism software (Version number 8.0, San Diego, CA).

In addition, RT-qPCR assay was also applied to analyze ASEs. We used a boundary-spanning primer for the sequence encompassing the junction of constitutive exon and alternative exon and an opposing primer in a constitutive exon in detecting alternative isoforms. The boundary-spanning primer of alternative exon was designed according to "model exon" to detect model splicing or according to "altered exon" to detect altered splicing. Primers for quantitative PCR analysis are presented in Table S1.

Availability of Data and Materials

The data discussed in this publication have been deposited in NCBI's Gene Expression Omnibus (GEO) and are accessible through GEO Series accession number GSE249957 (https://www.ncbi.nlm.nih.gov/geo/query/acc.cgi?acc=GSE249957).

Results

Quality Control of RNA Sample and Sequencing Data

BV2 cells were cultured and divided into control, OGD, and OGD + Acacetin groups. Total RNA extracted from these groups showed high concentration, purity, and integrity with quantities > 1 ug for all samples. This quality of RNA was crucial for successful library construction and high-throughput sequencing.

Sequencing of these samples yielded high-quality clean reads. As detailed in Table 1, the clean ratio for all samples is > 98.5%. Additionally, the proportion of bases with a sequencing error rate below 0.1% (Q30) > 94.9% across all samples. These results indicate that the sequencing data met the stringent criteria required for this study, thus ensuring the reliability and accuracy of the findings.

Table 1 Obtained the High-Quality Clean Reads

Sample ID	Raw read	Clean read	Ratio	Q20	Q30	GC
Control_1	69,532,280	68,506,235	98.52%	98.33%	94.93%	53%
Control_2	68,448,624	67,482,576	98.59%	98.28%	94.89%	53%
Control_3	68,618,646	67,685,788	98.64%	98.39%	95.05%	52%
Control_4	74,198,014	73,235,465	98.70%	98.35%	94.92%	52%
OGD_1	82,389,604	81,352,355	98.74%	98.42%	95.07%	52%
OGD_2	83,015,864	82,163,541	98.97%	98.38%	94.95%	55%
OGD_3	67,469,058	66,828,030	99.05%	98.27%	94.62%	56%
OGD_4	67,263,708	66,484,812	98.84%	98.41%	95.02%	52%
Acacetin_1	64,562,854	63,695,617	98.66%	98.41%	95.13%	52%
Acacetin_2	86,405,060	85,333,542	98.76%	98.36%	94.93%	52%
Acacetin_3	80,496,506	79,557,152	98.83%	98.42%	95.04%	51%
Acacetin_4	71,139,128	70,277,952	98.79%	98.40%	95.02%	52%

Notes: Q20, Base quality score indicating a sequencing error probability of less than 1%; Q30, Base quality score indicating a sequencing error probability of less than 0.1%; GC, The total percentage of guanine and cytosine in the sample.

Effects of Acacetin on DEGs in BV2 Microglia Following OGD/R Injury

Through the CCK-8 and LDH assays, we noticed that compared to the control group, the OGD/R-treated group exhibited a significant decrease in cell proliferation and an increase in LDH release. Conversely, acacetin treatment significantly enhanced cell proliferation and reduced LDH release (Figure 1A). RNA sequencing performed on the control, OGD/R, and OGD/R + Acacetin groups revealed distinct expression profiles among the groups, as indicated by a principal component analysis (PCA) and a heatmap of all mRNAs (Figure 1B–E). Compared with the control group, the OGD/R group showed 2148 upregulated and 2135 downregulated DEGs (Figure 1C). After the acacetin intervention, there were 240 upregulated and 248 downregulated DEGs (Figure 1D).

Functional Enrichment Analysis of DEGs

Compared to the control group, GO enrichment analysis revealed that the upregulated genes in the OGD/R group mainly participated in RNA splicing, mRNA processing, immune system processes, and nucleosome assembly (Figure 2A). KEGG pathway analysis further associated these genes with the spliceosome pathway (Figure S1A). Conversely, the downregulated genes were primarily enriched in GO terms fatty acid, glutathione, and lipid metabolism (Figure 2A). These genes, as determined by KEGG pathway analysis, were linked to the metabolic pathways of fatty acid and glutathione and the protective peroxisome pathway against oxidative damage (Figure S1B).

In the OGD/R-treated cells intervened with acacetin, GO enrichment analysis showed the upregulated genes were enriched in terms such as regulation of transcription, protein transport, cell cycle, and cell division (Figure 2B). KEGG analysis revealed their association with peroxisome and peroxisome proliferator-activated receptor (PPAR) signaling pathways (Figure S1C), which may contribute to maintaining intracellular redox balance. In contrast, the downregulated genes in GO enrichment analysis were primarily related to biological processes of nucleosome assembly, megakaryocyte differentiation, gene silencing, and transcription initiation (Figure 2B). Furthermore, KEGG pathway analysis emphasized their association with cytokine-cytokine receptor interaction and inflammation-related TNF and IL-17 signaling pathways (Figure S1D).

To delineate the impact of acacetin treatment on DEGs caused by OGD/R, an overlapping analysis was performed between DEGs from the OGD/R group and the acacetin group. It revealed that acacetin treatment reversed the expression

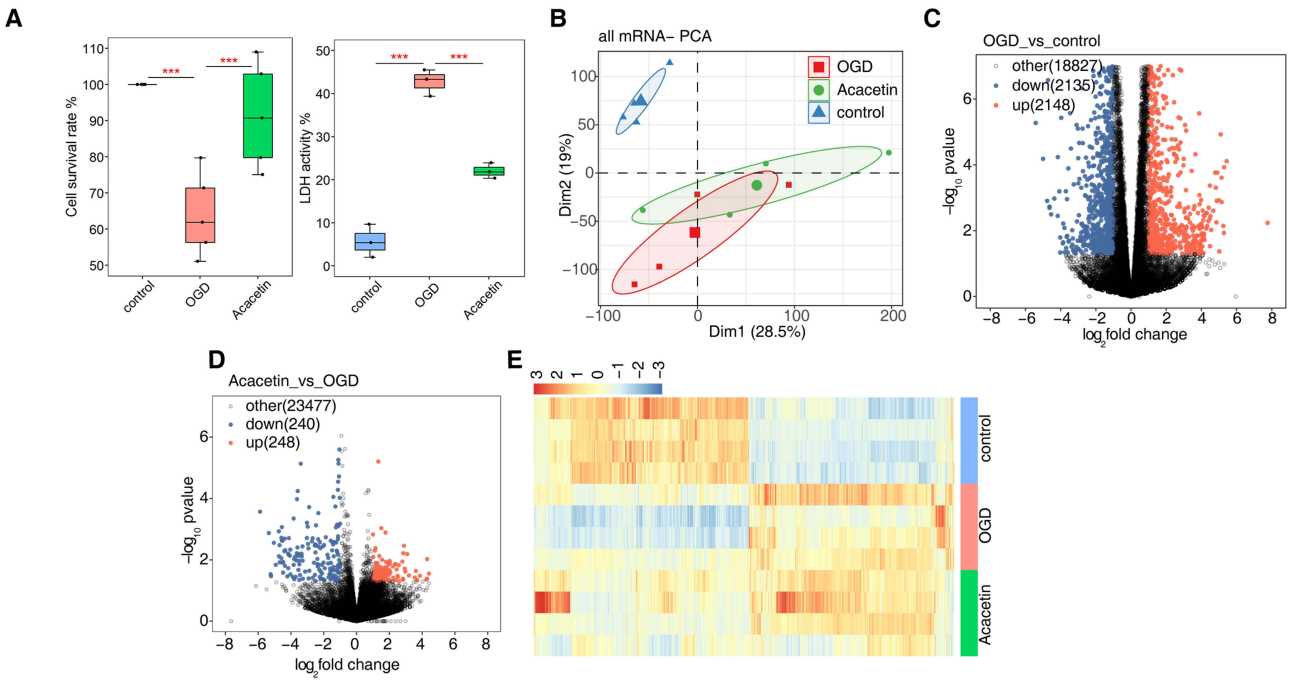

Figure 1 Effects on cell proliferation after treatment with OGD/R and intervention with acacetin, respectively. (**A**) Cell proliferation (**B**) PCA based on FPKM value of all detected genes. The ellipse for each group is the confidence ellipse. (**C**) Volcano plot showing all DEGs between OGD/R and control samples with DEseq2. P value < 0.05 and FC ≥ 1.5 or ≤ 0.67. (**D**) Volcano plot showing all DEGs between OGD/R and acacetin samples with DEseq2. P value < 0.05 and FC ≥ 1.5 or ≤ 0.67. (**E**) Hierarchical clustering heatmap showing FPKM of all DEGs. PCA, principal component analysis; OGD/R, oxygen glucose deprivation/re-oxygenation.

of 203 DEGs (Figure 2C and D), significantly downregulating 125 DEGs while upregulating 78 DEGs. Notably, genes involved in inflammatory signaling, such as Isg15, Fcgr1, Il1b, and Parp12, were markedly upregulated post-OGD/R but significantly downregulated after acacetin intervention. Additionally, the Mt2 gene, pertinent to the oxidative stress response, was considerably downregulated post-OGD/R but pronounced upregulated after acacetin intervention (Figure 2E). These findings were validated using RT-qPCR, and the results were highly consistent with our previous microarray data.

RASEs Analysis

Using RNA-seq data, we identified 1929 and 498 significant differential RASEs in the OGD/R and the acacetin intervened groups, respectively (Figure 3A and B). After OGD/R treatment, the genes involved in these RASEs, upon GO analysis, were primarily enriched in processes such as translation, cellular response, catalytic activity, and DNA repair (Figure 3C). KEGG pathway analysis further highlighted their associations with metabolic, longevity regulating, and ribosome pathways (Figure S2A). Following acacetin treatment, these genes were enriched in GO terms cell cycle, protein ubiquitination, cell division, and regulation of transcription (Figure 3C). KEGG pathways analysis linked these genes to fatty acid biosynthesis, p53 signaling, glucagon signaling, and ubiquitin-mediated proteolysis (Figure S2B). Upon an overlapping analysis of RASEs in significantly changed genes between OGD/R and acacetin intervention groups, we identified 68 overlapping differential RASEs (Figure 3D). Notably, a significant variation was observed in the A3SS event of the Trim47 gene, which is known to modulate apoptotic and inflammatory responses in cerebral IRI (Figure 3E). These results were validated by RT-qPCR, showing consistency with our previous microarray data.

lncRNA Analysis

Based on the RNA-seq data, we further analyzed the differentially expressed lncRNAs (DElncRNAs) after OGD/R treatment and acacetin intervention. Compared with the control group, we observed 385 lncRNAs upregulated and 355 downregulated in the OGD/R group. In contrast, in the acacetin group, we identified only 77 DElncRNAs compared to

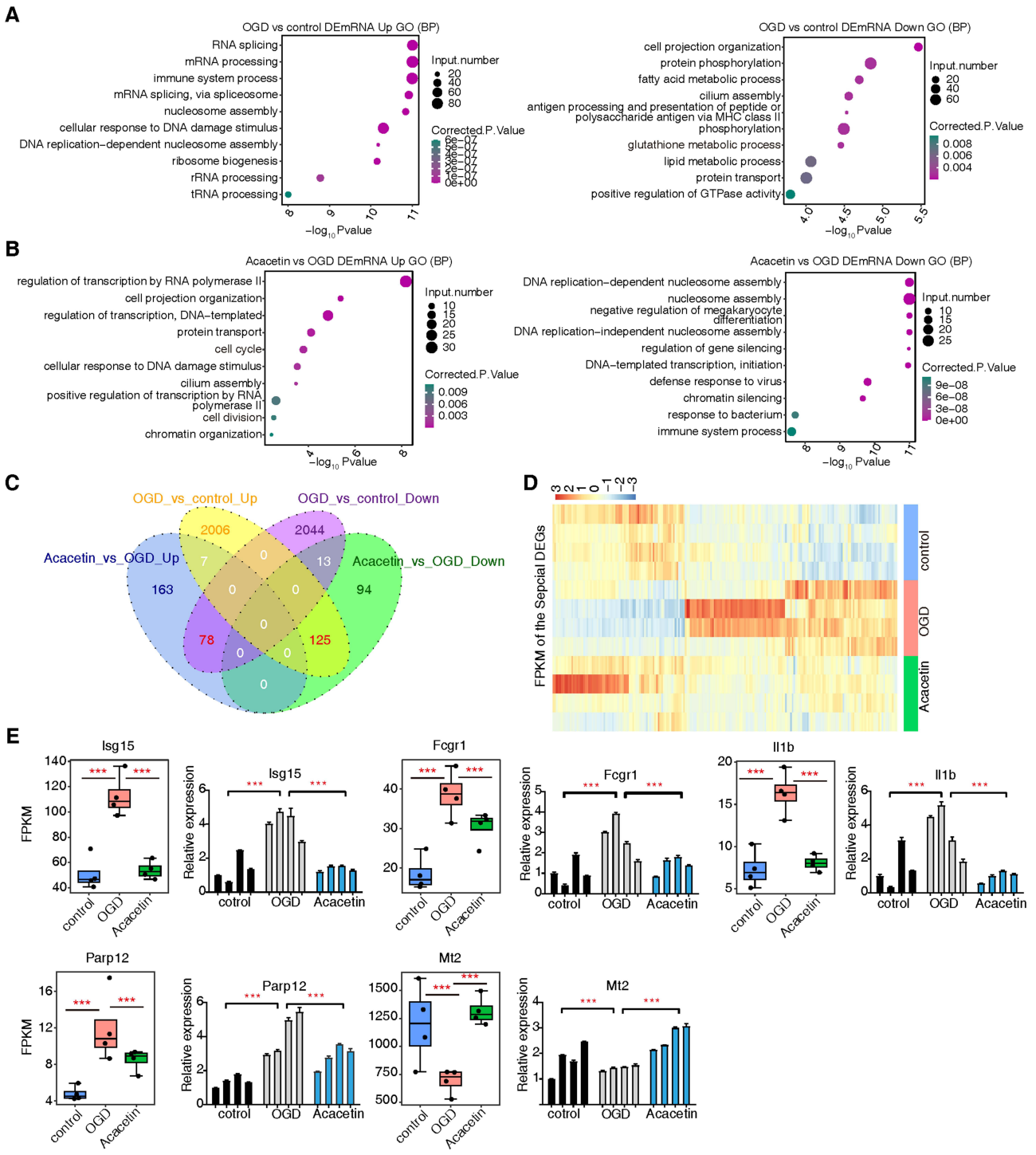

Figure 2 Acacetin regulates the expression of genes involved in inflammatory response and oxidative stress. (**A**) Bubble Diagram exhibiting the most enriched GO biological process results of the upregulated and down-regulated DEGs in the group OGD vs control. (**B**) Bubble Diagram exhibiting the most enriched GO biological process results of the upregulated and down-regulated DEGs in the group Acacetin vs OGD. (**C**) Venn diagram showing the overlap of up and down regulated DEGs between the group of OGD vs control and the group of Acacetin vs OGD. (**D**) Hierarchical clustering heatmap showing FPKM of the 78 and 125 DEGs in Figure 1C. (**E**) Boxplot showing the FPKM and statistical difference of the important genes. Bar plot shows the RNA-seq validation of these genes. Error bars represent mean ± SEM. *** P-value < 0.001.

the OGD/R group, with 40 upregulated and 37 downregulated (Figure 4A–C). An overlapping analysis of DElncRNAs across the three groups revealed that acacetin treatment resulted in downregulating 28 lncRNAs and upregulating 17 lncRNAs (Figure 4D). Notably, the lncRNAs Rmrp and Terc, both associated with neuroinflammation, were upregulated after OGD/R treatment but downregulated following acacetin intervention (Figure 4E and F). Moreover, GO analysis of

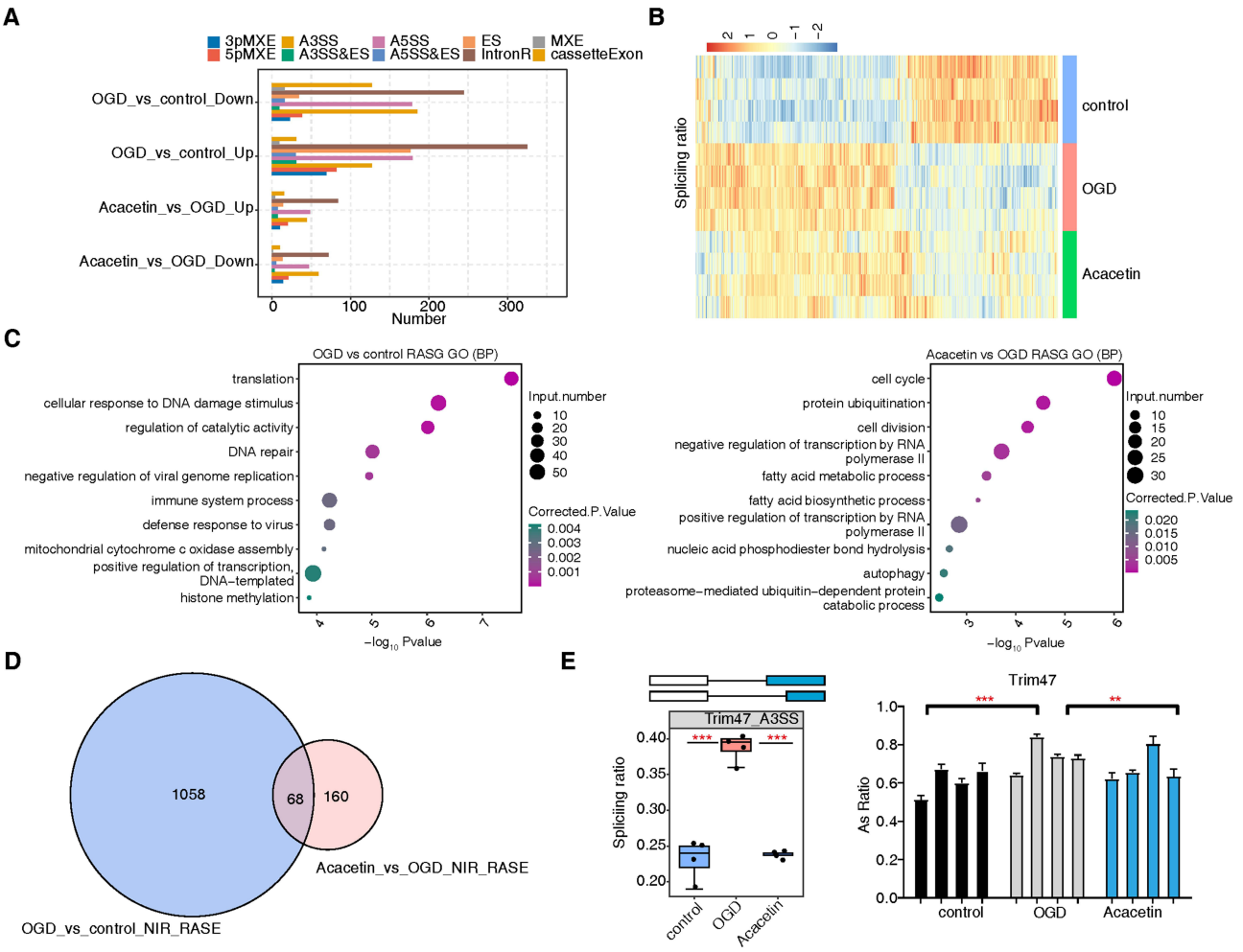

Figure 3 Acacetin regulates gene alternative splicing to prevent apoptosis and inflammatory activation. (**A**) Bar plot showing the number of all significant regulated alternative splicing events (RASEs). X-axis: RASE number. Y-axis: the different types of AS events. (**B**) Hierarchical clustering heatmap showing RASEs ratio. (**C**) Bubble Diagram exhibiting the most enriched GO biological process results of genes in the two groups. (**D**) Venn diagram showing the overlap of NIR RASEs between the group of OGD vs control and the group of Acacetin vs OGD. (**E**) Box plot shows the splicing ratio of Trim47_A3SS. Bar plot shows the RNA-seq validation of the RASE. Error bars represent mean ± SEM. ** P-value < 0.01, *** P-value < 0.001.

the co-expressed genes of DElncRNAs primarily showed enrichment in terms of nucleosome assembly, immune system process, and inflammatory response (Figure S3A, B). We hypothesize that Rmrp and Terc could mediate the transcription and expression levels of specific target genes (Figure 4G), which were mainly enriched in GO terms humoral and immune responses. Furthermore, members of the histone H2B family, including H2bc12, H2bc7, H2bc15, H2bc13, and H2bc11, were all upregulated after OGD/R treatment but downregulated after acacetin intervention (Figure S3C). Thus, Rmrp and Terc may modulate cellular immune and inflammatory responses through their differential expression.

Discussion

Acacetin has a protective effect against IRI, mitigating myocardial IRI by inhibiting oxidative stress and apoptosis, and reducing kidney damage induced by ischemia-reperfusion through its antioxidant properties.[20,21] Our previous study revealed that acacetin provides protective effects against cerebral IRI, though the underlying mechanisms remain to be elucidated.[4] Therefore, in this study, we used RNA-seq to explore the possible pathogenesis of the effects of acacetin on OGD/R injury in BV2 cells. We found the DEGs mainly associated with oxidative stress and inflammatory responses through GO enrichment analysis and KEGG pathway analysis. Overlapping analysis of the genes among the three groups

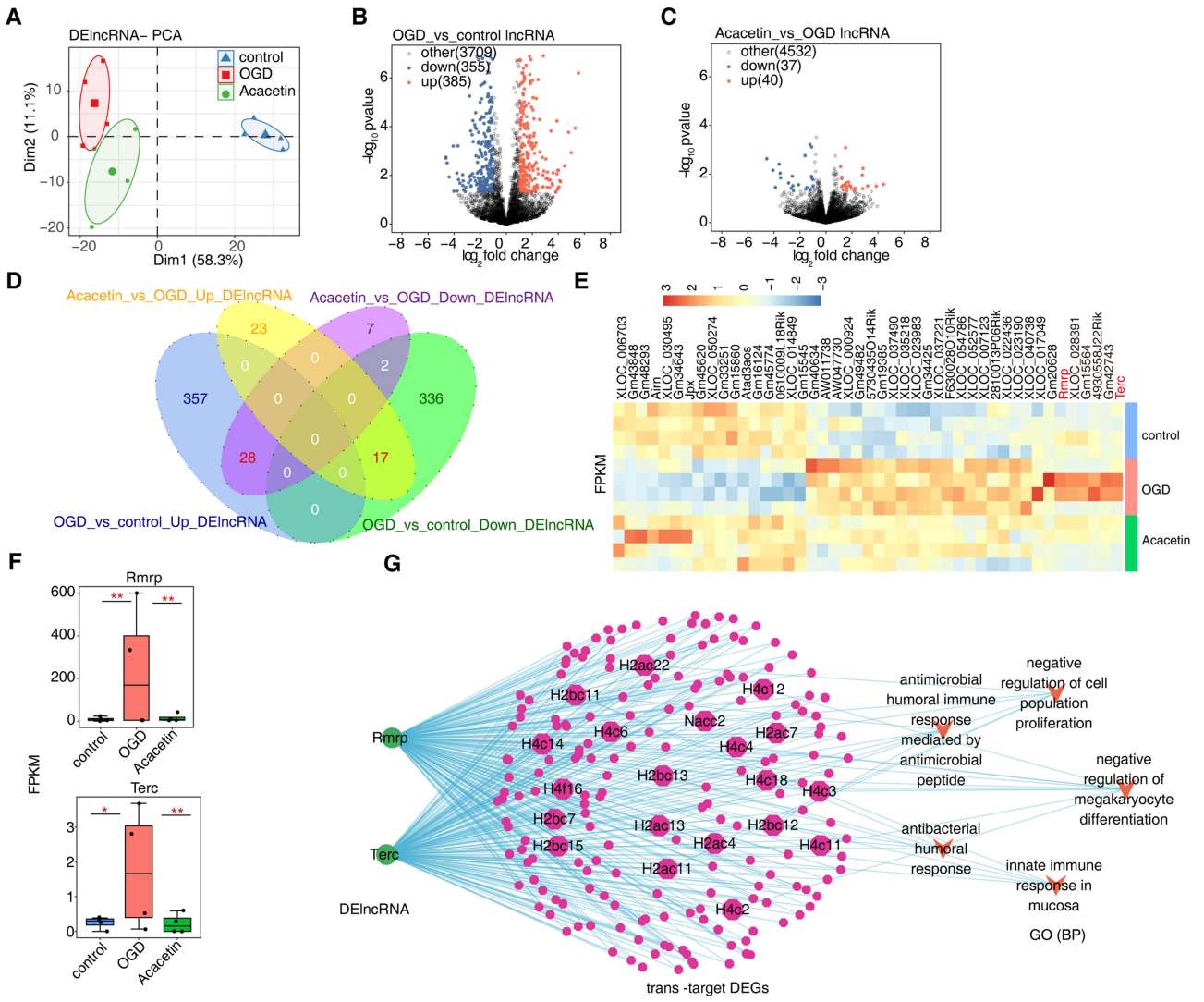

Figure 4 Acacetin regulates lncRNA expression to modulate inflammatory response. (**A**) PCA based on FPKM value of all detected DElncRNAs. The ellipse for each group is the confidence ellipse. (**B**) Volcano plot showing all differentially expressed DElncRNAs between OGD and control samples with DEseq2. P value < 0.05 and FC (fold change) ≥ 1.5 or ≤ 0.67. (**C**) Volcano plot showing all differentially expressed DElncRNAs between Acacetin and OGD samples with DEseq2. P value< 0.05 and FC (fold change) ≥ 1.5 or ≤ 0.67. (**D**) Venn diagram showing the overlap up and down DElncRNAs between the group of OGD vs control and the group of Acacetin vs OGD. (**E**) Hierarchical clustering heat map showing FPKM of the 28 and 17 DElncRNAs in (**D**). (**F**) Boxplot showing the FPKM and statistical difference of the important DElncRNAs Error bars represent mean ± SEM. * P-value < 0.05, ** P-value < 0.01. (**G**) Network diagram showing all trans target DEGs regulated by DElncRNAs Rmrp and Terc in the two groups.

revealed that acacetin significantly downregulated 125 genes and upregulated 78 genes. Notable among these were Isg15, Fcgr1, Il1b, Parp12, and Mt2, identified as pivotal genes potentially mediating the neuroprotective effects of acacetin.

The Isg15 gene encodes a ubiquitin-like protein known as ISG15, crucial in innate immune responses. Several studies demonstrated a significant increase of ISG15 in the brains of mice subjected to global ischemia and traumatic brain injury.[22,23] The Fcgr1 gene is responsible for encoding the cell surface receptor FcγRI, implicated in various immune responses. FcγRI in dorsal root ganglion neurons might enhance the synthesis and release of neuronal cytokines IL-1β and IL-18 through the NF-κB/NLRP3 pathway, triggering the activation of glial cells in the spinal dorsal horn and contributing to rheumatoid arthritis pain.[24] The Il1b gene is a critical mediator that plays a vital role in the cascade of inflammatory processes during reperfusion. Notably, our results revealed an upregulation in Il1b post-OGD/R injury, which was significantly reduced upon acacetin treatment. Our previous in vitro *and* in vivo experiments consistently showed augmented IL-1β expression after cerebral IRI, which acacetin intervention could significantly curtail.[25,26] Aberrant activity in PARP12 has been linked to various diseases, including inflammation, cardiovascular diseases, and

cancer.[27] PARP12 has been verified to colocalize and interact with members of the NF-κB signaling pathway.[28] Furthermore, overexpression of PARP12 activates NF-κB signaling, promoting IL-8 secretion in response to an extracellular ligand. However, the role of PARP12 in cerebral IRI remains unreported. Moreover, our findings showed a downregulation of the antioxidative stress-related gene, Mt2, after OGD/R injury, which was significantly upregulated post-acacetin intervention. It has been found that Mt2 could suppress TNF-α mRNA induction, protecting against ischemic injury in vitro and in vivo.[29]

OGD/R treatment and acacetin intervention may modulate inflammatory responses by regulating the alternative splicing of specific genes. After acacetin intervention in OGD/R-treated cells, genes that displayed significant changes in ASEs were primarily enriched in KEGG pathways fatty acid biosynthesis, p53 signaling, glucagon signaling, and ubiquitin-mediated proteolysis. Among these, the Trim47 gene, which underwent significant differential splicing events, regulates both cell apoptosis and inflammatory responses and is a crucial modulator in cerebral IRI. Silencing Trim47 could inhibit the NF-κB signaling pathway, mitigate inflammatory responses, suppress neuronal cell apoptosis, and ameliorate sevoflurane-induced neuronal cell injury and cognitive dysfunction in neonatal rats.[30] Meanwhile, TRIM47 expression in the brain and vasculature was inversely correlated with the severity of a wide range of small vessel diseases.[31] Furthermore, reducing Trim47 expression in vitro and in vivo has protective effects against cerebral IRI. It may be associated with the blockade of NF-κB signaling, the suppression of IL-6, TNF-α, and the release of inducible nitric oxide synthase (iNOS).[32]

In addition to regulating mRNA transcription, RNA-seq data revealed that both OGD/R treatment and acacetin intervention promote differential expression of numerous lncRNAs, potentially exerting effects by modulating target genes' transcription and expression levels. Notably, post-OGD/R treatment, the expression of lncRNA Rmrp and Terc was significantly upregulated, while it was markedly downregulated following acacetin intervention. LncRNA Rmrp competitively bound to miR-613, leading to an enhanced expression of ATG3 and the suppression of the JAK2/STAT3 pathway, thereby promoting cerebral IRI in mice.[33] Furthermore, the inhibition of lncRNA Terc, through the miR-34a-5p/XBP-1 axis, activates Akt and inhibits p-38, thereby mitigating neuronal apoptosis and inflammation in spinal cord injuries.[34] Hence, these lncRNAs might play a pivotal role in cerebral IRI by modulating the expression of target genes.

While our study has made notable progress, we recognize that several aspects require further investigation and enhancement. To explore the underlying mechanisms of acacetin in attenuating cerebral IRI, we established an OGD/R model, conducted transcriptome sequencing, and validated the expression of the Isg15, Fcgr1, Il1b, and Parp12 genes, as well as the A3SS splicing event in the Trim47 gene using RT-qPCR. However, additional experiments are necessary, such as employing Western Blot to detect the expression of these proteins and performing further validation in animal models.

Conclusion

In summary, acacetin may provide its protective effects against cerebral IRI by modulating the expression or alternative splicing of genes related to oxidative stress and inflammatory responses, thereby inhibiting intracellular inflammation. Furthermore, acacetin might function by regulating the expression of specific lncRNAs, which could mediate the differential expression of target genes. However, the precise underlying mechanisms require further experimental validation.

Funding

This work was supported by the Natural Science Foundation of Xinjiang Uygur Autonomous Region (Grant No. 2020D01C095); the "Tianshan Youth Project" of the Program for Fostering Excellent Young Talents in Science and Technology of Xinjiang Uygur Autonomous Region (Grant No. 2020Q046).

Disclosure

The authors report no conflicts of interest in this work.

References

1. Wang D, Ji X, Kang D, et al. Brief report on stroke center in China, 2020. *Chin J Cerebrovas Dis*. 2021;18(11):737–743. doi:10.3969/j.issn.1672-5921.2021.11.001
2. Lin L, Wang X, Yu Z. Ischemia-reperfusion injury in the brain: mechanisms and potential therapeutic strategies. *Biochem Pharmacol*. 2016;5(4):213. doi:10.4172/2167-0501.1000213
3. Ma Y, Wang J, Wang Y, Yang GY. The biphasic function of microglia in ischemic stroke. *Prog Neurobiol*. 2017;157:247–272. doi:10.1016/j.pneurobio.2016.01.005
4. Bu J, Shi S, Wang H, et al. Acacetin protects against cerebral ischemia-reperfusion injury via the NLRP3 signaling pathway. *Neural Regen Res*. 2019;14(4):605–612. doi:10.4103/1673-5374.247465
5. Hrdlickova R, Toloue M, Tian B. RNA-seq methods for transcriptome analysis. *Wiley Interdiscip Rev RNA*. 2017;8(1). doi:10.1002/wrna.1364
6. Wang Z, Gerstein M, Snyder M. RNA-seq: a revolutionary tool for transcriptomics. *Nat Rev Genet*. 2009;10(1):57–63. doi:10.1038/nrg2484
7. Li H, Wang Y, Wang B, et al. Baicalin and geniposide inhibit polarization and inflammatory injury of OGD/R-treated microglia by suppressing the 5-LOX/LTB4 pathway. *Neurochem Res*. 2021;46(7):1844–1858. doi:10.1007/s11064-021-03305-1
8. Kim D, Langmead B, Salzberg SL. HISAT: a fast spliced aligner with low memory requirements. *Nat Methods*. 2015;12(4):357–360. doi:10.1038/nmeth.3317
9. Trapnell C, Williams BA, Pertea G, et al. Transcript assembly and abundance estimation from RNA-seq reveals thousands of new transcripts and switching among isoforms. *Nat Biotechnol*. 2010;28(5):511–515. doi:10.1038/nbt.1621
10. Love MI, Huber W, Anders S. Moderated estimation of fold change and dispersion for RNA-seq data with DESeq2. *Genome Biol*. 2014;15(12):550. doi:10.1186/s13059-014-0550-8
11. Cheng C, Liu L, Bao Y, et al. Suva: splicing site usage variation analysis from RNA-seq data reveals highly conserved complex splicing biomarkers in liver cancer. *RNA Biol*. 2021:18(sup1):157–171. doi:10.1080/15476286.2021.1940037
12. Kovaka S, Zimin AV, Pertea GM, Razaghi R, Salzberg SL, Pertea M. Transcriptome assembly from long-read RNA-seq alignments with StringTie2. *Genome Biol*. 2019;20(1):278. doi:10.1186/s13059-019-1910-1
13. Wang L, Park HJ, Dasari S, Wang S, Kocher JP, Li W. CPAT: coding-potential assessment tool using an alignment-free logistic regression model. *Nucleic Acids Res*. 2013;41(6):e74–e74. doi:10.1093/nar/gkt006
14. Kong L, Zhang Y, Ye ZQ, et al. CPC: assess the protein-coding potential of transcripts using sequence features and support vector machine. *Nucleic Acids Res*. 2007;35(suppl_2):W345–W349. doi:10.1093/nar/gkm391
15. Wang G, Yin H, Li B, et al. Characterization and identification of long non-coding RNAs based on feature relationship. *Bioinformatics*. 2019;35(17):2949–2956. doi:10.1093/bioinformatics/btz008
16. Sun L, Luo H, Bu D, et al. Utilizing sequence intrinsic composition to classify protein-coding and long non-coding transcripts. *Nucleic Acids Res*. 2013;41(17):e166–e166. doi:10.1093/nar/gkt646
17. Yang R, Huang F, Fu J, et al. Differential transcription profiles of long non-coding RNAs in primary human brain microvascular endothelial cells in response to meningitic Escherichia coli. *Sci Rep*. 2016;6:38903. doi:10.1038/srep38903
18. Xie C, Mao X, Huang J, et al. KOBAS 2.0: a web server for annotation and identification of enriched pathways and diseases. *Nucleic Acids Res*. 2011;39(suppl_2):W316–W322. doi:10.1093/nar/gkr483
19. Livak KJ, Schmittgen TD. Analysis of relative gene expression data using real-time quantitative PCR and the 2−ΔΔCT method. *Methods*. 2001;25(4):402–408. doi:10.1006/meth.2001.1262
20. Shiravi A, Jalili C, Vaezi G, Ghanbari A, Alvani A. Acacetin attenuates renal damage-induced by ischemia-reperfusion with declining apoptosis and oxidative stress in mice. *Int J Prevent Med*. 2020;11:22. doi:10.4103/ijpvm.IJPVM_512_18
21. Wu C, Chen R, Wang Y, Wu W, Li G. Acacetin alleviates myocardial ischaemia/reperfusion injury by inhibiting oxidative stress and apoptosis via the nrf-2/HO-1 pathway. *Pharm Biol*. 2022;60(1):553–561. doi:10.1080/13880209.2022.2041675
22. He W, Wei D, Cai D, Chen S, Li S, Chen W. Altered long non-coding RNA transcriptomic profiles in ischemic stroke. *Hum Gene Ther*. 2018;29(6):719–732. doi:10.1089/hum.2017.064
23. Wang R, Kaul M, Zhang D. Interferon-stimulated gene 15 as a general marker for acute and chronic neuronal injuries. *Sheng Li Xue Bao*. 2012;64(5):577–583.
24. Liu F, Su S, Wang T, Yuan B, Ma C. Knocking out Fcgr1 of dorsal root ganglion attenuates the activation of NF-κB/NLRP3 pathway in a rat model of rheumatoid arthritis. *Basic Clinical Med*. 2021;41(7):963–969. doi:10.3969/j.issn.1001-6325.2021.07.006
25. Bu J, Zhang Y, Mahan Y, et al. Acacetin improves cognitive function of APP/PS1 Alzheimer's disease model mice via the NLRP3 inflammasome signaling pathway. *Transl Neurosci*. 2022;13(1):390–397. doi:10.1515/tnsci-2022-0254
26. Bu J, Ji G, Mahan Y, Wang Z, Wu X, Niu X. Acacetin protects against cerebral ischemia-reperfusion injury by regulating ROS/NLRP3 signaling pathway via autophagy. *J Apopl Nervous Dise*. 2023;40(2):99–102. doi:10.19845/j.cnki.zfysjjbzz.2023.0025
27. Almeleebia TM, Ahamad S, Ahmad I, et al. Identification of PARP12 inhibitors by virtual screening and molecular dynamics simulations. *Front Pharmacol*. 2022;13:847499. doi:10.3389/fphar.2022.847499
28. Ke Y, Zhang J, Lv X, Zeng X, Ba X. Novel insights into PARPs in gene expression: regulation of RNA metabolism. *Cell Mol Life Sci*. 2019;76(17):3283–3299. doi:10.1007/s00018-019-03120-6
29. Eidizadeh A, Khajehalichalehshtari M, Freyer D, Trendelenburg G. Assessment of the therapeutic potential of metallothionein-II application in focal cerebral ischemia in vitro and in vivo. *PLoS One*. 2015;10(12):e0144035. doi:10.1371/journal.pone.0144035
30. Zhu Y, Zhang M, Wang J, Wang Q. Knocking down trim47 ameliorated sevoflurane-induced neuronal cell injury and cognitive impairment in rats. *Exp Brain Res*. 2023;241(5):1437–1446. doi:10.1007/s00221-023-06602-z
31. Mishra A, Duplaà C, Vojinovic D, et al. Gene-mapping study of extremes of cerebral small vessel disease reveals TRIM47 as a strong candidate. *Brain*. 2022;145(6):1992–2007. doi:10.1093/brain/awab432

32. Hao M, Xie L, Leng W, Xue R. Trim47 is a critical regulator of cerebral ischemia-reperfusion injury through regulating apoptosis and inflammation. *Biochem Biophys Res Commun*. 2019;515(4):651–657. doi:10.1016/j.bbrc.2019.05.065
33. Wei L, Peng Y, Yang X, Zhou P. Knockdown of long non-coding RNA RMRP protects cerebral ischemia–reperfusion injury via the microRNA-613/ATG3 axis and the JAK2/STAT3 pathway. *Kaohsiung J Med Sci*. 2021;37(6):468–478. doi:10.1002/kjm2.12362
34. Ding W, Xu W, Lu D, et al. Inhibition of TERC inhibits neural apoptosis and inflammation in spinal cord injury through akt activation and p-38 inhibition via the miR-34a-5p/XBP-1 axis. *Open Med*. 2023;18(1). doi:10.1515/med-2022-0619